nature microbiology

Article

https://doi.org/10.1038/s41564-022-01318-2

# Restriction endonuclease cleavage of phage DNA enables resuscitation from Cas13-induced bacterial dormancy

Received: 28 June 2022

Accepted: 22 December 2022

Published online: 13 February 2023

Check for updates

Madison C. Williams[1,6], Alexandra E. Reker[1,6], Shally R. Margolis[1], Jingqiu Liao[2], Martin Wiedmann[3,4], Enrique R. Rojas[5] & Alexander J. Meeske[1]

Type VI CRISPR systems protect against phage infection using the RNA-guided nuclease Cas13 to recognize viral messenger RNA. Upon target recognition, Cas13 cleaves phage and host transcripts non-specifically, leading to cell dormancy that is incompatible with phage propagation. However, whether and how infected cells recover from dormancy is unclear. Here we show that type VI CRISPR and DNA-cleaving restriction-modification (RM) systems frequently co-occur and synergize to clear phage infections and resuscitate cells. In the natural type VI CRISPR host *Listeria seeligeri*, we show that RM cleaves the phage genome, thus removing the source of phage transcripts and enabling cells to recover from Cas13-induced cellular dormancy. We find that phage infections are neutralized more effectively when Cas13 and RM systems operate together. Our work reveals that type VI CRISPR immunity is cell-autonomous and non-abortive when paired with RM, and hints at other synergistic roles for the diverse host-directed immune systems in bacteria.

In response to phage predation, bacteria have evolved elaborate repertoires of antiviral defences that provide immunity through diverse mechanisms of action[1,2]. During infection, activities of prokaryotic immune effectors and the nature of the invading virus both influence the fate of the infected cell. While some effectors elicit cell survival by direct neutralization of the virus (termed cell-autonomous immunity), others work via abortive infection, initiating a growth arrest or programmed cell death response in the infected cell, which promotes survival of uninfected kin. Many bacteria encode both abortive and non-abortive defences; how their combined activities affect the outcome of infection is not well understood.

CRISPR-Cas systems use RNA-guided nucleases to provide sequence-specific immunity against foreign genetic elements, including phages[3], plasmids[4] and transposons[5]. While most CRISPR-Cas systems act by cleavage of phage DNA, the type VI CRISPR nuclease Cas13 exclusively recognizes and cleaves RNA[6]. We previously discovered that upon engagement with targeted phage messenger RNA, Cas13 is activated as a non-specific RNase and degrades both phage and host RNA in its natural host bacterium *Listeria seeligeri*[7]. Under these circumstances, cleavage of host RNAs results in a state of cellular dormancy incompatible with either continued cell growth or progression of the phage lytic cycle. Type VI CRISPR-Cas systems can provide robust antiviral immunity to a wide range of viruses through this abortive infection-like mechanism[6–10].

In addition to CRISPR immunity, approximately 74% of bacterial genomes encode restriction-modification (RM) systems that use restriction endonucleases to recognize and cleave 4–8 bp motifs on phage DNA[11–13]. Cleavage of phage DNA by RM systems

[1]Department of Microbiology, University of Washington, Seattle, WA, USA. [2]Department of Civil and Environmental Engineering, Virginia Tech, Blacksburg, VA, USA. [3]Department of Food Science, Cornell University, Ithaca, NY, USA. [4]Graduate Field of Microbiology, Cornell University, Ithaca, NY, USA. [5]Department of Biology, New York University, New York, NY, USA. [6]These authors contributed equally: Madison C. Williams and Alexandra E. Reker. e-mail: meeske@uw.edu

is generally thought to enable survival of the infected cell, making RM a cell-autonomous immune mechanism. Although many bacteria that encode type VI CRISPR systems probably also carry one or more RM systems, there has been no investigation into how the activities of these systems influence one another. Two reports have demonstrated that DNA-targeting CRISPR systems and RM can exert anti-phage immunity at the same time[14,15]. Previous investigations of type VI CRISPR immunity have been performed with methylated or otherwise restriction-resistant phages[6–10]. Here we find that RM systems frequently co-occur with type VI-A CRISPR systems in strains of *L. seeligeri* and other *Listeria*, and the two defences both operate during phage infection. Our data indicate that RM-mediated cleavage of phage genomes enables the survival and growth of infected cells, despite activation of non-specific RNA cleavage by Cas13. Finally, we observed that the clearance of phage DNA, neutralization of infection and cell growth after infection are all more effective in cells equipped with both RM and Cas13 than strains harbouring either defence alone. While type VI CRISPR systems can provide effective immunity through abortive infection, our work indicates that they also enhance the cell-autonomous immunity elicited by DNA-targeting defences.

## Results

### Type VI CRISPR and RM systems frequently co-occur

We recently established the natural type VI-A CRISPR host *L. seeligeri* as a genetically tractable model for studying Cas13a-based immunity[7,10,16]. To better understand the context in which type VI CRISPR systems function, we sequenced the genomes of 62 diverse isolates of *L. seeligeri* and evaluated their anti-phage defence system content. CRISPR and RM systems were the most well-represented defences (Extended Data Fig. 1a). We identified four CRISPR types in *L. seeligeri* (Fig. 1a): DNA-targeting type I-B (in 69% of genomes), type II-A (50%), type II-C (6%) loci as well as RNA-targeting type VI-A loci (in 29% of genomes). We observed these CRISPR loci in diverse combinations (Fig. 1b); while some strains possessed only one CRISPR type, most harboured multiple types, and no two types co-occurred with each other exclusively. While most DNA-targeting CRISPR loci were found in 1–2 hotspots across different genomes, type VI loci exhibited larger variation in location (Extended Data Fig. 1b). Our genomic analysis also indicated that 90% of the strains had one or more RM systems (Extended Data Fig. 1c,d). Collectively, these observations suggest that *L. seeligeri* strains possess a diverse complement of anti-phage defence loci located throughout the genome.

We next investigated whether any defence systems were closely associated with type VI CRISPR systems. We tallied the number of RM systems in each genome and discovered a statistically significant enrichment in average number of RM loci within genomes also harbouring type VI CRISPR loci (Fig. 1c). In contrast, we detected no significant difference in RM content for strains with type I-B or type II-A CRISPR loci (type II-C loci were too sparse for a meaningful comparison) (Extended Data Fig. 1e). In addition to a higher number of RM loci, we found that 100% of *L. seeligeri* strains with type VI CRISPR harboured at least one RM system (Fig. 1d). Next, we expanded our analysis to include 943 *Listeria* genomes available in the NCBI whole-genome sequencing database. Among these genomes, we detected a smaller but still statistically significant enrichment in RM co-occurrence and count in strains containing a type VI system. Finally, we analysed the RM content of 90 diverse species representing all known hosts of type VI-A, VI-B, VI-C and VI-D CRISPR systems, and found that 96% of them harbour at least one RM system (average, 2.95 RM loci; Supplementary Table 1). These bioinformatic analyses suggest that most type VI CRISPR loci could perform anti-phage defence in concert with one or more DNA-targeting RM systems.

### *L. seeligeri* LS1 has two functional type I RM systems

To investigate whether the RM systems we identified function in anti-phage immunity, we performed phage-challenge experiments in our most well-characterized strain, *L. seeligeri* LS1. The LS1 genome encodes two type I RM systems, which are each transcribed at levels comparable to the CRISPR locus as well as other genes expressed during exponential growth (Extended Data Fig. 2). We deleted each RM locus individually and also generated a double deletion. We performed efficiency-of-plaquing assays in which we challenged each of these mutants and wild-type (WT) LS1 with five different listeriaphages from our collection: A118, ϕEGDe, U153, ϕLS46 and ϕLS59 (Fig. 2a). LS1 has type I-B and type VI-A CRISPR-Cas systems but does not carry any spacers matching any of the phages tested, therefore CRISPR immunity was not activated during these experiments. Each RM system reduced plaquing efficiency for all five phages. Compared with the double RM deletion, the individual RM systems conferred between a 2-fold and 500-fold degree of protection, and both systems together provided an equal or greater level of immunity depending on the phage. We performed PacBio sequencing of the LS1 genome in strains possessing each RM system individually to identify RM recognition sites. We aligned the sequences surrounding methylated adenines to generate consensus recognition motifs (Fig. 2b and Supplementary Files 1 and 2). Consistent with other type I RM sites[12], these motifs are each composed of two 4–5 basepair motifs separated by 7–8 random nucleotides. When we tallied the number of sites present in the genomes of the phages used for efficiency-of-plaquing assays, we observed a statistically significant correlation between the number of RM sites and the degree of anti-phage defence (Fig. 2c,d). Collectively, these data indicate that both type I RM systems of *L. seeligeri* LS1 use target site recognition to perform anti-phage defence against a variety of phages.

### Cells armed with RM and type VI CRISPR survive infection

During type VI CRISPR immunity, Cas13 recognition of crRNA-complementary phage messenger RNA triggers non-specific cleavage of both phage and host RNAs, leading to dormancy of the infected cell[6,7]. As the RNase activity of Cas13 does not eliminate the phage DNA, which is the source of target RNA, infected cells remain in stasis. We therefore hypothesized that RM cleavage of phage genomes might allow infected cells to escape Cas13-induced dormancy. Alternatively, triggering Cas13 activity might result in irreversible commitment to cell dormancy, regardless of phage genome elimination by RM. To explore this idea, we grew cultures of WT LS1 and the double RM deletion mutant in the presence or absence of a type VI spacer targeting the restriction-sensitive phage ϕLS59 and measured the number of viable colony-forming units (c.f.u.) before and at 0.5, 4 and 24 h post-infection (Fig. 3a). The lysis time of ϕLS59 is 2 h, therefore the c.f.u. measurement at 0.5 h reflects the fates of the initially infected cells. We used a high multiplicity of infection (MOI = 10) to ensure that most cells were infected. We performed this experiment with two different spacers, one targeting an early-transcribed ϕLS59 lytic gene (spcE), and one targeting a late-transcribed gene (spcL), each of which provide robust immunity against ϕLS59 (Extended Data Fig. 3). We observed an initial ~50-fold reduction in c.f.u. after infecting cells lacking RM immunity, regardless of the presence of a targeting spacer, indicating that infected cells are mostly unable to form viable colonies. After 24 h, while ΔRM cultures with a non-targeting spacer lysed to near completion, cultures with a targeting spacer recovered and proliferated. In contrast, all three of the WT strains containing RM systems (with or without spcE and spcL) maintained viability after infection, and all continued to proliferate over the time course. We observed a similar survival phenotype during infection by a different phage, A118, in the presence of both RM and an early-targeting spacer (Fig. 3b). These results suggest that cells endowed with both RM and type VI CRISPR immunity largely survive infection.

We considered that cells equipped with both RM and type VI CRISPR immunity could survive phage infection by two mechanisms: (1) RM nucleases could cleave the phage genome before transcription of the phage lytic genes, therefore Cas13 activity would never be

https://doi.org/10.1038/s41564-022-01318-2

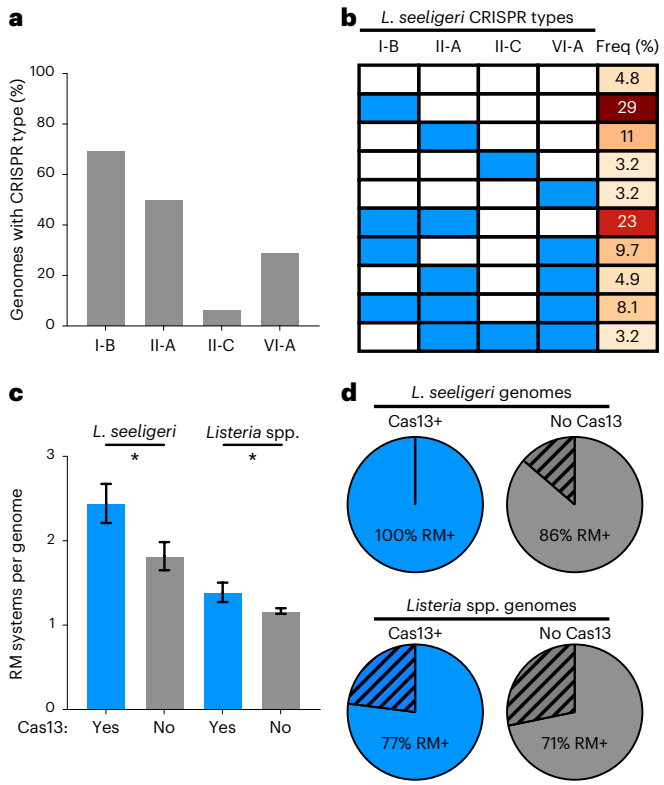


**Fig. 1 | Type VI-A CRISPR systems frequently co-occur with RM systems in *Listeria* genomes. a**, Percentage of 62 *L. seeligeri* genomes harbouring the indicated CRISPR type. **b**, Combinations of CRISPR loci observed in 62 *L. seeligeri* genomes. Filled blue rectangles indicate the presence of the indicated CRISPR type. Darker red color represents higher frequency of the indicated CRISPR type combination. **c**, Average tally of RM systems per genome. **d**, Percentage of genomes containing any RM loci in *Listeria* strains with or without Cas13. *L. seeligeri* genomes (62) and 943 genomes from a broader dataset of *Listeria* spp. were analysed. Error bars denote s.e.m. Asterisks denote statistical significance (*L. seeligeri*: $P = 0.0411$, *Listeria* spp.: $P = 0.0472$) using unpaired Student's *t*-test (two-tailed).

triggered and the cells would not enter dormancy or (2) phage lytic gene transcription, Cas13 activation and cell dormancy all precede phage genome cleavage by RM nucleases, but elimination of the phage genome allows the cell to be resuscitated. To distinguish between these possibilities, we determined whether Cas13 is activated in the presence of RM immunity during phage infection. First, we analysed cell growth rates during ϕLS59 infection of cells containing RM, type VI targeting spacers, or both (Fig. 3c). We infected cells at MOI 10 and tracked culture growth (by optical density $(OD)_{600}$) over a period of 24 h. Cells lacking both RM and CRISPR immunity were lysed by the phage and did not recover within the growth period. In contrast, cells harbouring RM but with a non-targeting spacer grew at rates indistinguishable from uninfected cells. The strains lacking RM but armed with a type VI spacer initially exhibited severe growth defects after infection, but later recovered. Our c.f.u. measurements indicated that most infected cells in this population were unable to form colonies, therefore uninfected cells were probably responsible for the eventual regrowth of the culture, as p.f.u. were reduced from the culture, and isolates that survived the infection had no evolved phage receptor mutations or became lysogens (Extended Data Fig. 4). Finally, while the strain containing both RM and spcL exhibited unperturbed growth, we observed a small but reproducible lag in growth after infection of the strain containing both RM and spcE. Consistent with these measurements, we noted a similar trend in our c.f.u. measurements (Fig. 3a) at 4 h post-infection: the WT $RM^+$ strain with either a non-targeting spacer or spcL proliferated more at this time point than the strain armed with spcE. These results suggest that cells equipped with spcE trigger Cas13 immunity and cell dormancy before RM systems can clear infecting phage genomes.

To directly test whether Cas13 is activated during ϕLS59 infection in the presence of RM systems, we performed northern blots that enabled us to monitor Cas13-mediated RNA cleavage over time in vivo. We blotted for the *L. seeligeri* 5S ribosomal RNA, which we previously demonstrated to be a substrate of Cas13[16]. In the absence of RM or CRISPR immunity, we observed a single prominent 5S ribosomal RNA (rRNA) band throughout the course of infection. For strains lacking RM but carrying a type VI targeting spacer, we observed the formation of lower molecular weight cleavage products after phage infection. The onset of cleavage depended on the timing of target transcript expression: for spcE, cleavage was evident at 5 min post-infection; for spcL, cleavage was delayed until 60 min post-infection. In contrast, in the WT $RM^+$ strains with either a non-targeting spacer or spcL, 5S rRNA remained intact for at least 4 h after infection, mirroring the growth curve data in Fig. 3c and suggesting that Cas13 was not activated in these strains. Finally, the $RM^+$ strain harbouring spcE exhibited rapid-onset cleavage of 5S rRNA after infection, indicating that Cas13 is activated before RM-mediated clearance of the phage genome. Importantly, the extent of cleavage was similar for $spcE^+$ cells, regardless of the presence of RM, suggesting a similar degree of Cas13 activity in both strains. We also noted the formation of higher molecular weight bands during later timepoints in the $RM^+$ $spcE^+$ cells. We hypothesize that these bands represent the precursor rRNAs that are processed to generate mature 5S rRNA[17]. The accumulation of these intermediates may be a consequence of resuscitation from Cas13-induced dormancy. Collectively, these results suggest that type VI CRISPR immunity precedes RM cleavage of the phage genome when activated by an early-transcribed target, but phage DNA degradation prevents the production of late-transcribed targets. Furthermore, our observation of cell survival despite Cas13 activation during infection of the $RM^+$ $spcE^+$ strain suggests that RM-mediated cleavage of the phage genome allows cells to exit Cas13-induced dormancy.

## RM cleavage of phage genomes reverses Cas13 dormancy

To directly test whether RM systems allow exit from Cas13-mediated cell dormancy, we monitored the growth of single cells after infection via microscopy. We used ϕLS59 to infect WT and ΔRM strains with or without a targeting spacer at an MOI 10. Then, we loaded infected cells into microfluidic chambers where they were trapped for imaging. After a 10 min adsorption period, we washed out unbound phage with growth medium, which was supplied continuously throughout the experiment. To ensure that the majority of cells were stably infected under these conditions, we labelled ϕLS59 by soaking in SYTOX-Green (Fig. 4a). During the early stages of infection with labelled phage, fluorescent phage particles were visible at the cell periphery. Within 20 min, infected cells exhibited bright cytosolic fluorescence as a consequence of injection of the labelled phage genome. When we imaged cells infected at MOI 10, virtually every cell contained fluorescent label (Fig. 4b). Next, we monitored cell growth for 5 h after infection with unlabelled phage. After infection, we observed 4 distinct phenotypes (Fig. 4c,d). Cells lacking RM and CRISPR grew unperturbed, but almost always lysed within 3 h after infection. In contrast, ΔRM cells containing spcE exhibited rapid growth arrest. While nearly every cell ceased growth, 23% eventually lysed during the timelapse, suggesting that Cas13-induced dormancy can be lethal under some circumstances. In the presence of RM immunity alone, nearly all cells grew and divided normally after infection, and only rarely lysed or entered stasis. Finally, $RM^+$ cells armed with spcE exhibited a range of phenotypes in our experiments. While 36% of the cells grew without delay, 32% underwent transient growth arrest but then resumed growth. Finally, 27% remained in a state of arrest

https://doi.org/10.1038/s41564-022-01318-2

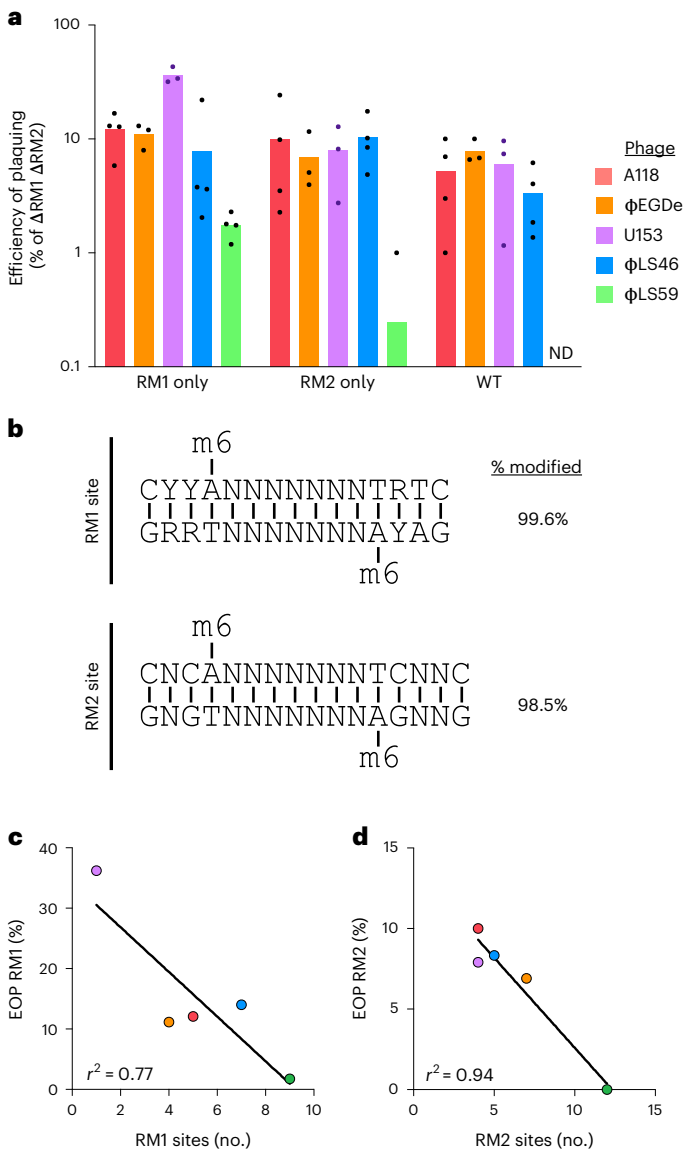


**Fig. 2 | *L. seeligeri* LS1 encodes two functional type I RM systems. a**, Efficiency of plaquing (EOP) assay testing the ability of five different phages to infect LS1 strains with 0, 1 or 2 RM systems. EOP values for each phage are reported as a percentage of the number of plaques formed on LS1 lacking both RM systems (ΔRM1 ΔRM2). All phage stocks were prepared from infections of the ΔRM1 ΔRM2 strain. ND, not detected. Axis intercept represents limit of detection. **b**, Type I RM recognition motifs for LS1 RM1 and RM2 systems identified by PacBio sequencing. 6-methyl adenine modifications were detected at the indicated consensus motifs in genomic DNA purified from LS1 lacking RM2 (to identify the RM1 site) or lacking RM1 (to identify the RM2 site). The percentages of methylated genomic motifs matching the consensus are indicated on the right. Y, pyrimidine, R, purine. **c**, Negative correlation between the number of RM1 recognition sites on phage genomes and the mean EOP for that phage on bacteria harbouring RM1. Each phage is colour-coded as in **a**. Correlation coefficient ($r^2$) shown, statistically significant by two-tailed Pearson's correlation test ($P = 0.049$). **d**, Same as **c**, but for RM2 ($P = 0.0061$).

throughout the imaging period. We noted two forms of recovery from dormancy that would each result in the formation of a viable colony: (1) infected cells that underwent delayed growth, then began elongating and dividing again (Fig. 4c, 4th column) and (2) infected cells that divided into two daughter cells, one of which continued growth, while the other stayed in arrest (Fig. 4c, 5th column). These microscopy data directly demonstrate that cells can use RM immunity to survive the collateral effects of Cas13 RNase activities during type VI CRISPR immunity.

We hypothesized that RM systems enable escape from Cas13-mediated dormancy by eliminating phage DNA. Therefore, we tracked the presence of ϕLS59 DNA after infection with a fluorescent reporter-operator system (FROS)[18] using an mCherry-labelled allele of the DNA binding protein TetR and its 19 bp binding motif *tetO*. We generated a ϕLS59 mutant harbouring an array of 60 *tetO* sites inserted downstream of the late lytic genes. We confirmed that this mutant phage retained sensitivity to both RM and Cas13 immunity (Extended Data Fig. 5). In the absence of phage infection, we observed a uniformly distributed cytosolic fluorescent signal in cells carrying a plasmid-encoded tetR-mCherry (Fig. 4e). Next, we infected ΔRM cells without a targeting spacer using ϕLS59 tetOx60. After infection, the tetR-mCherry signal in most cells coalesced into 1–2 foci that were usually positioned towards the cell poles and remained stable over the course of infection (Fig. 4e,f and Extended Data Fig. 6). When we infected a ΔRM strain equipped with spcE and tetR-mCherry, we observed a similar degree of stable phage genome foci formation, suggesting that Cas13 immunity is insufficient to eliminate the phage genome. In contrast, when we infected RM$^+$ cells with ϕLS59 tetOx60, we observed unstable phage DNA foci that were cleared within 15–20 min, consistent with our observations that Cas13 activation by an early-targeting spacer (which happens by 5 min post-infection) precedes RM cleavage of the phage genome (Extended Data Fig. 6). Most RM$^+$ cells did not exhibit phage genome foci at 40 min post-infection, instead displaying diffuse cytosolic fluorescence similar to our observations of uninfected cells. Notably, we did observe instances of stable phage genome foci in 5% of RM$^+$ cells lacking Cas13 immunity. Phage genome foci were even rarer (1% of cells) in RM$^+$ spcE cells, suggesting that although Cas13 does not directly interfere with phage DNA, Cas13 activities enhance the clearance of phage DNA during RM immunity. Collectively, these observations indicate that Cas13 activity does not lead to an irreversible stasis in cell growth, but RM clearance of phage genomes allows survival and recovery from Cas13-induced dormancy during type VI CRISPR immunity.

## Anti-phage synergy between RM and type VI CRISPR systems

While the results described above demonstrate that RM and Cas13 immunity both operate during the same phage infection, they do not explain what advantage type VI CRISPR immunity might confer to bacteria already armed with RM. On the contrary, Cas13-induced dormancy actually elicited a growth disadvantage during infection with ϕLS59 (Fig. 3c). To investigate this, we measured the number of productive phage infections using a centre of infection (COI) assay (Fig. 5a). We infected WT and ΔRM cells with or without spcE with ϕLS59 at MOI 10, washed them to remove remaining phage particles, then plated the infected cells (centres of infection) on a lawn of phage-sensitive ΔRM cells lacking CRISPR. In this assay, infected cells that successfully produce even a single phage particle will give rise to a detectable plaque. Despite our observation that ϕLS59 does not form plaques on WT LS1 (Fig. 2a), we observed that ϕLS59 productively infects ~1% of cells containing either RM or Cas13+spcE alone. In contrast, we were unable to detect any successful infections of cells harbouring both RM and type VI CRISPR immunity. Thus, while Cas13 immunity elicits a growth defect during anti-phage immunity, it synergizes with RM in phage neutralization.

Next, we wondered whether Cas13 might provide a more pronounced benefit during infection by phages that are less RM-sensitive. Of the phages we examined, ϕLS59 is by far the most RM-sensitive, with 21 RM recognition sites in its genome. Therefore, we examined infection efficiency and cell growth during infection by the slightly more RM-resistant phage A118, which has only 9 RM sites in its genome and is targeted by a naturally occurring type VI spacer (Extended Data Fig. 7a). We confirmed that A118 is sensitive to Cas13 targeting, with a

https://doi.org/10.1038/s41564-022-01318-2

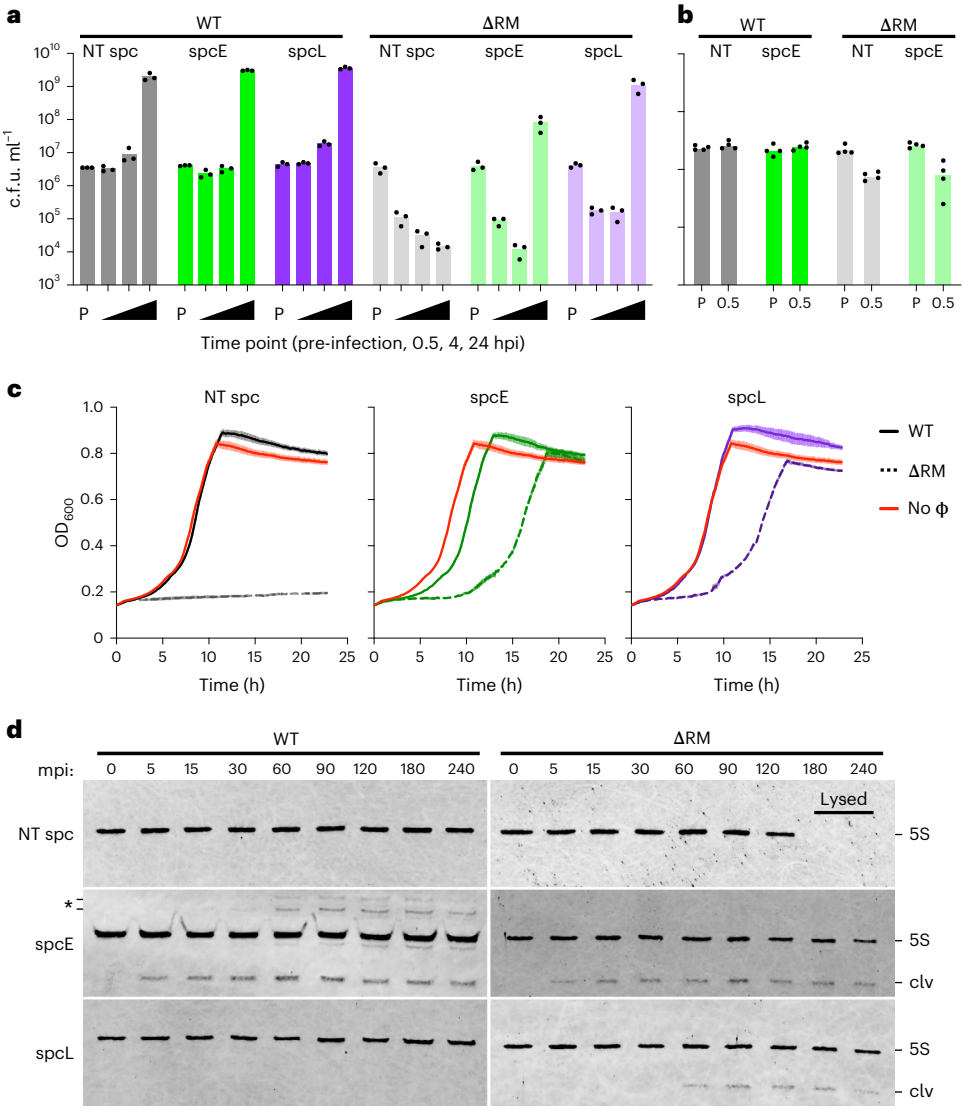


**Fig. 3 | Cells armed with RM and type VI CRISPR survive infection. a**, Viable c.f.u. count during ϕLS59 infection of *L. seeligeri* LS1. Cells of the indicated genotype were infected with ϕLS59 at MOI 10. Viable c.f.u. were enumerated before infection (P), as well as 0.5, 4 and 24 h post-infection. NT, non-targeting spacer; spcE, spacer targeting early lytic gene; spcL, spacer targeting late lytic gene. Analysis of 3 biological replicates is shown. **b**, C.f.u. count during A118 infection of LS1 at MOI 10. **c**, Growth curves during ϕLS59 infection of LS1. Strains of the indicated genotype were infected at MOI = 10, $OD_{600}$ = 0.01. $OD_{600}$ was monitored for 24 h after infection. Solid lines indicate WT $RM^+$ strains, dashed lines indicate ΔRM strains. Uninfected controls are shown in red. Error bars represent s.e.m from 3 biological replicates. **d**, Northern blot analysis of 5S rRNA cleavage during type VI CRISPR immunity. Strains of the indicated genotype were infected with ϕLS59 at MOI 10, then RNA was extracted and probed for 5S rRNA. Cas13-dependent cleavage products (clv) and putative rRNA precursors (*) are shown. Representative of two biological replicates.

spacer targeting an early lytic gene (spcE) (Extended Data Fig. 7b). As expected, we observed a higher rate of RM escape for A118 in the COI assay (Fig. 5a). As with ϕLS59, A118 was unable to productively infect cells equipped with both RM and Cas13 immunity. Next, we monitored growth in liquid culture by optical density during A118 infection, as in Fig. 3c. In contrast to the unperturbed growth we observed for $RM^+$ cells during ϕLS59 infection (Fig. 3c), the same strain rapidly succumbed to A118 infection (Fig. 5b). The strain lacking RM but armed with spcE exhibited a prolonged growth defect during A118 infection. However, the strain with both RM and spcE began to recover from infection after 10 h. When we performed the infection at MOI 1, we observed the same pattern of protection among the four strains; while a strain with RM alone exhibited temporary protection from infection, and the strain with spcE alone recovered after a growth defect, the strain with both RM and spcE grew unperturbed (Extended Data Fig. 7c). The enhanced survival of the $RM^+$ spcE strain in these experiments indicates that Cas13 confers a protective advantage to bacteria infected by phage whose sensitivity to RM interference is incomplete.

## Discussion

Here we have investigated the fates of bacteria that use both abortive infection and cell-autonomous immunity to combat phage infection. Previous reports have established that type VI CRISPR systems unleash non-specific RNA degradation activity upon recognition of targeted phage transcripts, which leads to growth cessation[6,7]. Thus, a prevalent model held that type VI CRISPR immunity exclusively acts through an abortive infection mechanism in which the infected cell does not recover but restricts the propagation of phage, protecting uninfected cells in the greater population. In this study, we have shown that the natural type VI CRISPR host *L. seeligeri* interferes with phage

https://doi.org/10.1038/s41564-022-01318-2

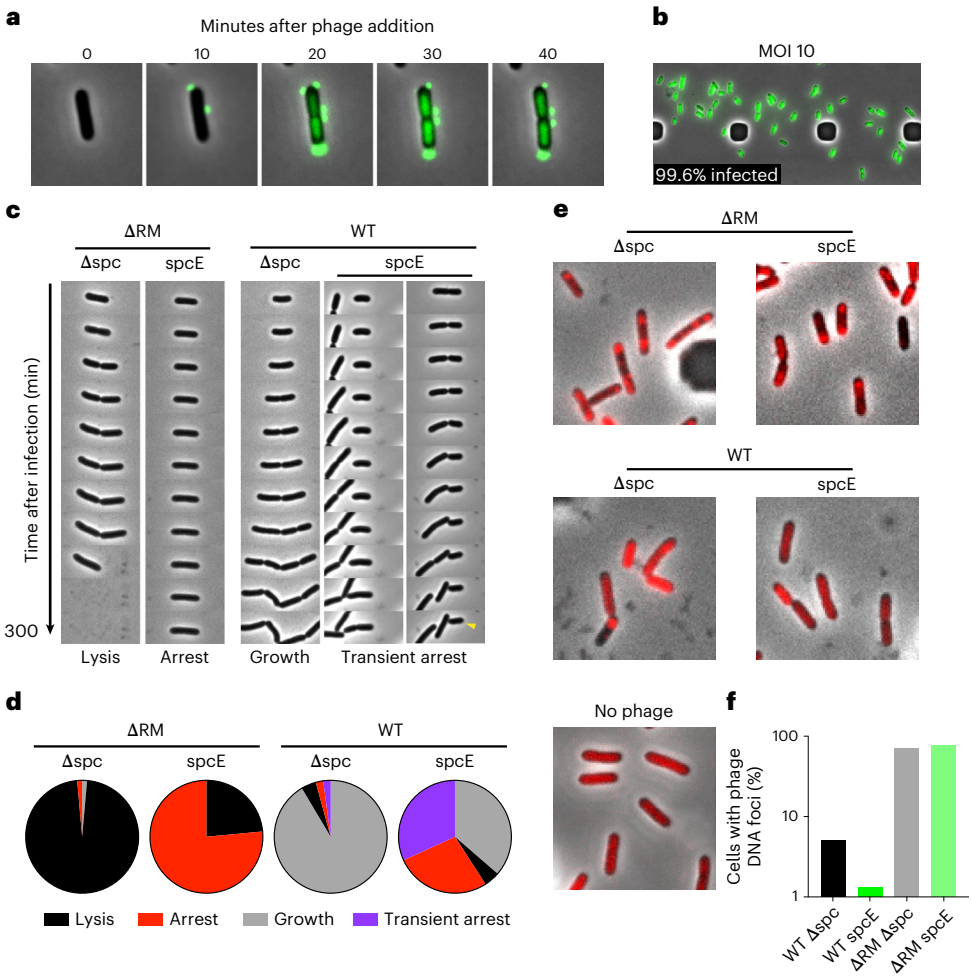


**Fig. 4 | RM cleavage of phage genomes enables recovery from Cas13-induced cell dormancy. a**, Timelapse montage of LS1 cells infected with SYTOX-Green-labelled ϕLS59 in a microfluidic chamber. Overlay of SYTOX-Green signal and phase contrast images. **b**, Field of cells infected with SYTOX-Green-labelled ϕLS59 at MOI 10 and loaded into microfluidic chamber. The four dark areas are features of the microfluidic device. Percent infection quantified from 314 cells. **c**, Timelapse montage examples showing cells of the indicated genotype during growth in a microfluidic chamber after ϕLS59 infection. The fate of each cell is indicated at the bottom. For WT + *spcE*, two example phenotypes are shown. Left: a cell exhibiting delayed growth. Right: a cell that divides into a growing daughter and a dormant daughter (indicated with yellow caret). **d**, Percentage of cells exhibiting the indicated fate for each genotype. A total of 500 cells were analysed for each genotype. **e**, Representative images from FROS experiments tracking ϕLS59 DNA during infection. LS1 cells harbouring tetR-mCherry were infected with ϕLS59 tetOx60 and imaged at 40 min post-infection. **f**, Quantitation of data in **e** as percentage of cells of each genotype with detectable phage DNA foci. A total of 500 cells were analysed for each genotype.

infection using both Cas13 and RM systems. Under these circumstances, Cas13 activity and cell dormancy can be triggered while phage genome cleavage by RM is still underway. When this happens, the cell is not irreversibly committed to dormancy. Instead, the phage genome is cleared from the cell, removing the source of target transcripts, and the cell resumes growth (see Supplementary Discussion). Our data further indicate that cells armed with both immune systems exhibit stronger defence against phage infection. We conclude that, if paired with a DNA-targeting effector, type VI CRISPR systems can provide non-abortive immunity. While our data support the idea that RM systems can resolve the type VI immune response in *L. seeligeri*, it is also possible that other DNA-targeting immune systems, including additional CRISPR types, could play a similar role. However, co-targeting of a single phage by two CRISPR types would require either each CRISPR locus to be armed with a targeting spacer (possibly through coordinated adaptation), or sharing of crRNAs between the two types.

Finally, a multitude of different anti-phage defences beyond type VI CRISPR have been reported to operate via abortive infection[19]. These systems use diverse mechanisms to sense phage infection and respond by inducing growth arrest or cell death. For example, the *toxIN* toxin-antitoxin system of Gram-negative bacteria induces endoribonucleolytic cleavage of host and phage transcripts in response to shutdown of host transcription during phage infection[20,21]. While some abortive infection systems do result in cell death, our results provide experimental evidence for the proposal that cells using non-lethal abortive infection mechanisms might also resume growth when working in concert with additional defences[2,22]. Whether cells have the capacity to reverse the activities of different abortive infection systems probably depends on the infection-associated signals responsible for triggering the collateral activities of immune effectors, and the ability of those signals to be resolved by other anti-phage defences. These properties could therefore underlie synergistic relationships between diverse host-directed defence modules.

## Methods

### Bacterial strains and growth conditions

*L. seeligeri* strains were propagated in Brain Heart Infusion (BHI) broth or agar at 30 °C. Where appropriate, BHI was supplemented

https://doi.org/10.1038/s41564-022-01318-2

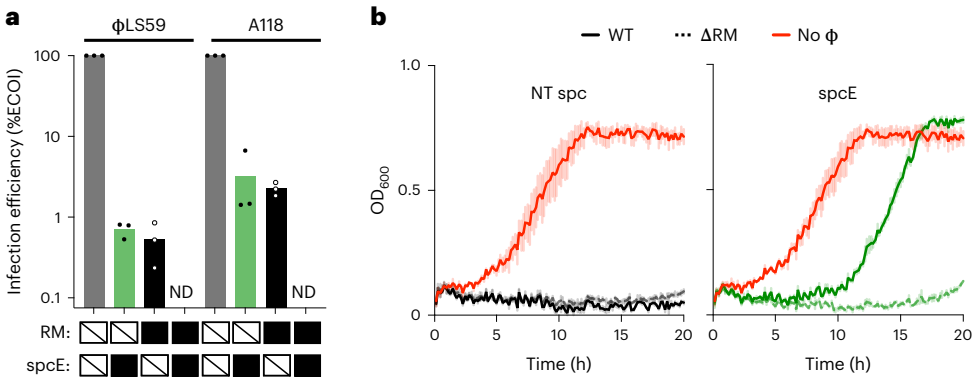


**Fig. 5 | RM and type VI CRISPR systems synergize in anti-phage immunity.** **a**, COI measurements for strains with (black boxes) or without (strikes) indicated defence. Cells were infected with the indicated phage at MOI 10 for 5 min, then washed 3 times before plating on a lawn of ΔRM cells lacking CRISPR. Infection efficiency reported as a percentage of the number of p.f.u. detected in the ΔRM non-targeting spacer infection. Axis intercept represents limit of detection. **b**, Growth curves during A118 infection of LS1. Strains of the indicated genotype were infected at MOI = 10, $OD_{600}$ = 0.01. $OD_{600}$ was monitored for 20 h after infection. Solid lines indicate WT $RM^+$ strains. Dashed lines indicate ΔRM strains. Uninfected controls are shown in red. Error bars are s.e.m. from 3 biological replicates.

with the following antibiotics for selection: nalidixic acid (50 μg $ml^{-1}$), chloramphenicol (10 μg $ml^{-1}$), erythromycin (1 μg $ml^{-1}$) or kanamycin (50 μg $ml^{-1}$). For cloning, plasmid preparation and conjugative plasmid transfer, *Escherichia coli* strains were cultured in Lysogeny Broth (LB) medium at 37 °C. Where appropriate, LB was supplemented with the following antibiotics: ampicillin (100 μg $ml^{-1}$), chloramphenicol (25 μg $ml^{-1}$) or kanamycin (50 μg $ml^{-1}$). For conjugative transfer of *E. coli–Listeria* shuttle vectors, plasmids were purified from Turbo Competent *E. coli* (New England Biolabs) and transformed into the *E. coli* conjugative donor strains SM10 λ*pir* or S-17 λ*pir*[23].

**Phage propagation.** Unless otherwise stated, all phage infections were performed in BHI medium supplemented with 5 mM $CaCl_2$. To generate phage lysates, existing phage stocks were diluted to single plaques on a lawn of *L. seeligeri* LS1 *ΔRM1 ΔRM2*, and a single plaque was purified twice to ensure homogeneity. Cell culture (5 ml) was infected with phage at MOI 0.1 and $OD_{600}$ 0.1, and the infection proceeded overnight. The lysate was centrifuged for 20 min at 4,000 × *g*, then the supernatant was filtered using a 0.45 μm pore syringe filter.

**Plasmid construction and preparation.** All genetic constructs for expression in *L. seeligeri* were cloned into the following three compatible shuttle vectors, each of which contains an origin of transfer sequence for mobilization by transfer genes of the IncP-type plasmid RP4. These transfer genes are integrated into the genome of the *E. coli* conjugative donor strains SM10 λ*pir* and S-17 λ*pir*[23]. All plasmids used in this study, along with details of their construction, can be found in Supplementary Table 2.

pPL2e: single-copy plasmid conferring erythromycin resistance that integrates into the $tRNA^{Arg}$ locus in the *L. seeligeri* chromosome[24].

pAM8: *E. coli–Listeria* shuttle vector conferring chloramphenicol resistance[16].

pAM326: *E. coli–Listeria* shuttle vector conferring kanamycin resistance[10].

**COI assay.** *L. seeligeri* strains were grown to mid-exponential phase, and 0.5 ml of culture at $OD_{600}$ 0.5 was infected with phage at MOI 10. Adsorption was carried out for 20 min. To remove unbound phage, the cell suspension was washed 3 times with 1 ml BHI and transferred to a fresh tube during the third wash. The samples were resuspended to a final volume of 1 ml. Infective centres were enumerated by measuring p.f.u. titre on a lawn of naïve *L. seeligeri* LS1 ΔRM1 ΔRM2.

**Adsorption assay.** *L. seeligeri* strains were grown to mid-exponential phase, and 0.5 ml of culture at $OD_{600}$ 0.5 was infected with phage at MOI 0.1. The same amount of phage was also added to an aliquot of media containing no cells. Adsorption was carried out for 20 min at room temperature, then the cells and bound phage were pelleted by centrifugation at 8,000 × *g* for 1 min. Samples of each supernatant (representing unbound phage) were collected, and p.f.u. were enumerated from each sample by titration on a lawn of naïve *L. seeligeri* LS1 ΔRM1 ΔRM2. The % adsorption was calculated as follows: $\%\text{Adsorption} = 100 \times (1 - (\text{p.f.u.}_{\text{Sample}})/(\text{p.f.u.}_{\text{NoCells}}))$

***E. coli–L. seeligeri* conjugation.** All genetic constructs for expression in *L. seeligeri* were introduced by conjugation with the *E. coli* donor strains SM10 λ*pir*, S-17 λ*pir*[23], or for allelic exchange (see below), β2163 Δ*dapA*[25]. Donor cultures were grown overnight in LB medium supplemented with the appropriate antibiotic (25 μg $ml^{-1}$ chloramphenicol for pPL2e-derived plasmids, 100 μg $ml^{-1}$ ampicillin for pAM8-derived plasmids, or 50 μg $ml^{-1}$ kanamycin for pAM326-derived plasmids) at 37 °C. Recipient cultures were grown overnight in BHI medium supplemented with the appropriate antibiotic (1 μg $ml^{-1}$ erythromycin for pPL2e-derived plasmids, 10 μg $ml^{-1}$ chloramphenicol for pAM8-derived plasmids, 50 μg $ml^{-1}$ kanamycin for pAM326-derived plasmids) at 30 °C. Donor and recipient cultures (100 μl each) were diluted into 10 ml of BHI medium and concentrated onto a filter disc (Millipore-Sigma, HAWP04700) using vacuum filtration. Filter discs were laid onto BHI agar supplemented with 8 μg $ml^{-1}$ oxacillin (which weakens the cell wall and enhances conjugation) and incubated at 37 °C for 4 h. Discs were removed, cells were resuspended in 2 ml BHI, and transconjugants were selected on medium containing 50 μg $ml^{-1}$ nalidixic acid (which kills donor *E. coli* but not recipient *L. seeligeri*) in addition to the appropriate antibiotic for plasmid selection. Transconjugants were isolated after 2–3 d incubation at 30 °C.

**Gene deletions and replacements in *Listeria*.** Allelic exchange plasmids were generated by cloning 1 kb homology arms flanking the genomic region to be deleted into the suicide vector pAM215[7], which does not replicate in *Listeria*, and contains a chloramphenicol resistance cassette and *lacZ* from *Geobacillus stearothermophilus*. These plasmids were then transformed into the *E. coli* donor strain β2163 Δ*dapA*[25], which is auxotrophic for diaminopimelic acid (DAP), selecting on LB medium supplemented with the appropriate antibiotic and 1.2 mM DAP. Conjugation was carried out as described above,

except that all steps were carried out in the presence of 1.2 mM DAP. Transconjugants were selected on media lacking DAP and containing 50 μg ml$^{-1}$ nalidixic acid to ensure complete killing of donor *E. coli*, as well as 10 μg ml$^{-1}$ chloramphenicol to select for integration of the pAM215-derived plasmid. Chloramphenicol-resistant colonies were patched on BHI supplemented with 100 μg ml$^{-1}$ 5-bromo-4-chloro-3-indolyl β-D-galactopyranoside (X-gal) and *lacZ*$^{+}$ was confirmed by checking for blue colony colour. Plasmid integrants were passaged 3–4 times in BHI at 30 °C in the absence of antibiotic selection to permit loss of the integrated plasmid. Cultures were screened for plasmid excision by dilution and plating on BHI + X-gal. White colonies were checked for chloramphenicol sensitivity, then chromosomal DNA was prepared from each and tested for the desired deletion by PCR using primers flanking the deletion site. Deletions were confirmed by Sanger sequencing.

**Type VI spacer cloning and expression in *L. seeligeri*.** All spacers used in this study were cloned into entry vector pAM305, which is a site-specific chromosomally integrating vector containing a type VI repeat-spacer-repeat miniarray expressed from the native promoter, with BsaI restriction sites in the spacer allowing for facile replacement. All strains used in this study have the native 5 spacer array deleted from the type VI CRISPR locus (with the promoter and *cas13* gene left intact). Spacer constructs were integrated into the genome via conjugation and expressed as the sole type VI spacer.

**Bacterial genome sequencing and assembly.** Chromosomal DNA was prepared from each *L. seeligeri* isolate by lysozyme digestion of the cell wall, followed by cell lysis with 1% sarkosyl, then phenol-chloroform extraction and ethanol precipitation. Chromosomal DNA (1 ng) was used to make an NGS library using the Illumina Nextera XT DNA Library Preparation kit according to the manufacturer's instructions. Library quality was confirmed by analysis on Agilent TapeStation, then 2x150 bp paired-end sequencing was carried out on the Illumina NextSeq platform. Raw reads were quality-trimmed with Sickle v1.0 (https://github.com/najoshi/sickle) using a quality cut-off of 30 and length cut-off of 45. Trimmed reads were assembled using SPAdes v3.15.4 (http://cab.spbu.ru/software/spades/) with default parameters, which resulted in assembled contigs. These contigs were mapped onto the completed reference genome of *L. seeligeri* SLCC3954 using Medusa (http://combo.dbe.unifi.it/medusa/) with default parameters, generating scaffold assemblies. In each draft genome assembly, only one scaffold represented the fully assembled genome.

**Construction of ϕLS59 tetOx60.** The tetOx60 array was inserted into the ϕLS59 genome by homologous recombination and Cas9 selection. A recombination template plasmid (pAM542) was generated containing the tetOx60 array flanked on each side by 500 bp of ϕLS59 sequence. The insertion site was downstream of the late lytic genes, in a putative accessory region of the genome. The insertion site lay adjacent to a protospacer-adjacent motif for SpyCas9, which we mutated in the recombination template to confer Cas9 resistance to recombinants. The recombination template plasmid pAM542 was introduced into LS1 ΔRM; this strain was infected with ϕLS59 in BHI top agar (allowing recombinants to be generated), and a phage stock was collected. A Cas9 spacer targeting the site disrupted by tetOx60 insertion was cloned into pAM307 to generate pAM545 and introduced into LS1 ΔRM. The ϕLS59 stock passaged on LS1 ΔRM carrying the pAM542 repair template was used to infect LS1 ΔRM carrying pAM545, and Cas9-resistant escaper mutants were isolated. Two mutant phage isolates were Sanger sequenced across the tetOx60 insertion site and found to contain the precise insertion.

**SYTOX-Green phage labelling.** Bacteriophage ϕLS59 was labelled by diluting phage stocks (at a titre of $1 \times 10^7$ p.f.u. μl$^{-1}$) 10-fold in SM buffer (100 mM NaCl, 50 mM Tris pH 7.5, 8 mM $MgSO_4$) containing 1 μM SYTOX-Green. Labelled phage were incubated at 4 °C overnight. For use in microscopy, phage were further diluted 10-fold in BHI containing 2 mM $CaCl_2$ before infection, then combined with *L. seeligeri* suspensions at MOI 10.

**Microscopy.** Timelapse imaging of phage infection was performed with mid-exponential phase cells infected at $OD_{600}$ 0.01 and MOI 10 in BHI medium supplemented with 2 mM $CaCl_2$. Adsorption was allowed to occur for 10 min, then cells were loaded into microfluidic chambers using the CellASIC ONIX2 microfluidic system (Millipore-Sigma). After cells became trapped in the chamber, they were supplied with BHI medium under a constant flow of 5 μl h$^{-1}$. Phase contrast images were captured at ×1,000 magnification every 10 min for 5 h after infection, using a Nikon Ti2e inverted microscope equipped with a Hamamatsu Orca-Fusion SCMOS camera and the temperature-controlled enclosure set to 30 °C. SYTOX-Green stain was imaged using a GFP filter set and TetR-mCherry signal with Texas Red filter set, both using an Excelitas Xylis LED Illuminator set to 6% power, with an exposure time of 300 ms. Timelapse images were aligned and processed using NIS Elements software v5.3. Quantitative analysis of cell fates and phage genome foci were performed in Fiji v2.3.0[26].

**Bioinformatics.** CRISPR-cas loci and RM loci were identified in *Listeria* genomes via TBLASTN searches of the 62 newly sequenced *L. seeligeri* genomes, as well as all *Listeriaceae* in the NCBI 'wgs' database (excluding *L. monocytogenes*). Cas proteins from each CRISPR type were used as queries for CRISPR loci, with a *E*-value cut-off of $10^{-4}$. For RM loci, all unique *Listeria* RM systems available on REBASE (rebase.neb.com) were used as queries in the TBLASTN searches above. Non-CRISPR anti-phage defence systems of the 62 *L. seeligeri* genomes were identified using PADLOC[27]; only systems containing all required genes are reported. To normalize genome positions, *dnaA* homologues were identified in each genome, and defence positions in Extended Data Fig. 1 are reported relative to each *dnaA* gene.

**C.f.u. survival assay.** Mid-exponential phase cells were diluted to $OD_{600}$ 0.005 in BHI medium supplemented with 5 mM $CaCl_2$, and a pre-infection sample was collected for c.f.u. enumeration. Cells were infected with phage at MOI 10, and additional c.f.u. samples were collected at 0.5, 4 and 24 h post-infection. Tenfold serial dilutions in BHI (8) were made from culture samples at the time of collection, and 5 μl of each dilution was spotted on BHI agar plates supplemented with 50 mM sodium citrate to prevent additional infections from occurring on the plate. Viable colonies were counted after 2 d incubation at 30 °C. C.f.u. values were graphed using GraphPad Prism v9.

**Methylation site identification.** Genome-wide methylation motifs on LS1 DNA were identified by PacBio sequencing of genomic DNA collected from LS1 ΔRM1 (to identify the RM2 methylation motif) and LS1 ΔRM2 (to identify the RM1 methylation motif). Sequencing was performed by CD Genomics. Methylation sites were identified using the BaseMod Analysis tool in the SMRT Analysis package, with assistance from the University of Washington PacBio Sequencing Center.

**RNA isolation and northern blot analysis.** Cultures (12 ml) of *L. seeligeri* strains were infected with ϕLS59 at MOI 10 and $OD_{600}$ 0.1. At indicated timepoints post-infection, 1 ml aliquots of culture were pelleted by centrifugation at 8,000 × *g* at 4 °C and frozen. Cell pellets were resuspended in 80 μl RNase-free PBS and lysed by a 5 min treatment with lysozyme at 20 μg ml$^{-1}$, followed by the addition of 1% sarkosyl. RNA was purified from these lysates by adding 300 μl Trizol LS (Thermo Fisher), followed by 80 μl chloroform. Samples were centrifuged at 15,000 × *g* for 15 min, and RNA was precipitated from the upper aqueous phase by the addition of glycoBlue co-precipitate and 200 μl isopropanol. RNA pellets were washed with 500 μl 80% ethanol,

air-dried and resuspended in RNase-free water. For northern blot analysis, 1 µg RNA per sample was diluted in RNA loading dye (95% formamide, 1.8 mM EDTA, 0.5% bromophenol blue), heated at 95 °C for 3 min, cooled on ice for 1 min and separated by gel electrophoresis on a precast 15% polyacrylamide denaturing TBE-urea gel. RNA was transferred to an Invitrogen Immobilon Ny+ nylon membrane using a Bio-Rad Mini Trans-Blot Cell filled with 1X TBE. RNA was fixed to membranes using an Analytik Jena UV crosslinker (optimal crosslinking setting). Membranes were pre-hybridized for 30 min at 42 °C in 2X SSC containing 1% SDS. Cy3-labelled single-stranded DNA probe (250 pmol) complementary to the 5S rRNA (oAM734) was hybridized to the membrane overnight at 42 °C. Membranes were washed twice with 2X SSC 0.1% SDS, once with 1X SSC 0.1% SDS, then imaged using an Azure Sapphire biomolecular imager with Sapphire Capture software (v1.0).

### Reporting summary

Further information on research design is available in the Nature Portfolio Reporting Summary linked to this article.

## Data availability

All *L. seeligeri* genome sequences reported here have been uploaded to NCBI through Genbank under BioProject accession number PRJNA901958. RM loci are publically available through the REBASE database (rebase.neb.com). Lists of strains, plasmids and oligonucleotides used in this study are available in Supplementary Table 2. Further information and requests for resources and reagents should be directed to and will be fulfilled by the corresponding author. Source data are provided with this paper.

## References


1. Tal, N. & Sorek, R. SnapShot: bacterial immunity. *Cell* **185**, 578-578.e1 (2022).
2. Rostol, J. T. & Marraffini, L. (Ph)ighting phages: how bacteria resist their parasites. *Cell Host Microbe* **25**, 184–194 (2019).
3. Barrangou, R. et al. CRISPR provides acquired resistance against viruses in prokaryotes. *Science* **315**, 1709–1712 (2007).
4. Marraffini, L. A. & Sontheimer, E. J. CRISPR interference limits horizontal gene transfer in staphylococci by targeting DNA. *Science* **322**, 1843–1845 (2008).
5. Watanabe, T. et al. CRISPR regulation of intraspecies diversification by limiting IS transposition and intercellular recombination. *Genome Biol. Evol.* **5**, 1099–1114 (2013).
6. Abudayyeh, O. O. et al. C2c2 is a single-component programmable RNA-guided RNA-targeting CRISPR effector. *Science* **353**, aaf5573 (2016).
7. Meeske, A. J., Nakandakari-Higa, S. & Marraffini, L. A. Cas13-induced cellular dormancy prevents the rise of CRISPR-resistant bacteriophage. *Nature* **570**, 241–245 (2019).
8. Mendoza, S. D. et al. A bacteriophage nucleus-like compartment shields DNA from CRISPR nucleases. *Nature* **577**, 244–248 (2020).
9. Adler, B. A. et al. Broad-spectrum CRISPR-Cas13a enables efficient phage genome editing. *Nat. Microbiol.* **7**, 1967–1979 (2022).
10. Meeske, A. J. et al. A phage-encoded anti-CRISPR enables complete evasion of type VI-A CRISPR-Cas immunity. *Science* **369**, 54–59 (2020).
11. Oliveira, P. H., Touchon, M. & Rocha, E. P. The interplay of restriction-modification systems with mobile genetic elements and their prokaryotic hosts. *Nucleic Acids Res.* **42**, 10618–10631 (2014).
12. Bickle, T. A. & Krüger, D. Biology of DNA restriction. *Microbiol. Rev.* **57**, 434–450 (1993).
13. Arber, W. Host-controlled modification of bacteriophage. *Annu. Rev. Microbiol.* **19**, 365–378 (1965).
14. Dupuis, M. E., Villion, M., Magadan, A. H. & Moineau, S. CRISPR-Cas and restriction-modification systems are compatible and increase phage resistance. *Nat. Commun.* **4**, 2087 (2013).
15. Maguin, P., Varble, A., Modell, J. W. & Marraffini, L. A. Cleavage of viral DNA by restriction endonucleases stimulates the type II CRISPR-Cas immune response. *Mol. Cell* **82**, 907–919.e7 (2022).
16. Meeske, A. J. & Marraffini, L. A. RNA guide complementarity prevents self-targeting in type VI CRISPR systems. *Mol. Cell* **71**, 791–801.e3 (2018).
17. Deutscher, M. P. Maturation and degradation of ribosomal RNA in bacteria. *Prog. Mol. Biol. Transl. Sci.* **85**, 369–391 (2009).
18. Robinett, C. C. et al. In vivo localization of DNA sequences and visualization of large-scale chromatin organization using lac operator/repressor recognition. *J. Cell Biol.* **135**, 1685–1700 (1996).
19. Bernheim, A. & Sorek, R. The pan-immune system of bacteria: antiviral defence as a community resource. *Nat. Rev. Microbiol.* **18**, 113–119 (2020).
20. Guegler, C. K. & Laub, M. T. Shutoff of host transcription triggers a toxin-antitoxin system to cleave phage RNA and abort infection. *Mol. Cell* **81**, 2361–2373.e9 (2021).
21. Fineran, P. C. et al. The phage abortive infection system, ToxIN, functions as a protein-RNA toxin-antitoxin pair. *Proc. Natl Acad. Sci. USA* **106**, 894–899 (2009).
22. Makarova, K. S., Anantharaman, V., Aravind, L. & Koonin, E. V. Live virus-free or die: coupling of antivirus immunity and programmed suicide or dormancy in prokaryotes. *Biol. Direct* **7**, 40 (2012).
23. Simon, R., Priefer, U. & Puhler, A. A broad host range mobilization system for in vivo genetic-engineering: transposon mutagenesis in Gram-negative bacteria. *Biotechnology* **1**, 784–791 (1983).
24. Lauer, P., Chow, M. Y., Loessner, M. J., Portnoy, D. A. & Calendar, R. Construction, characterization, and use of two *Listeria monocytogenes* site-specific phage integration vectors. *J. Bacteriol.* **184**, 4177–4186 (2002).
25. Demarre, G. et al. A new family of mobilizable suicide plasmids based on broad host range R388 plasmid (IncW) and RP4 plasmid (IncPalpha) conjugative machineries and their cognate *Escherichia coli* host strains. *Res. Microbiol.* **156**, 245–255 (2005).
26. Schindelin, J. et al. Fiji: an open-source platform for biological-image analysis. *Nat. Methods* **9**, 676–682 (2012).
27. Payne, L. J. et al. Identification and classification of antiviral defence systems in bacteria and archaea with PADLOC reveals new system types. *Nucleic Acids Res.* **49**, 10868–10878 (2021).


## Acknowledgements

We thank all members of the Meeske lab for advice and encouragement, members of the Guo and Mitchell labs for helpful discussions, R. Calendar (UC Berkeley) for providing A118 and U153 phages, and D. Rudner (Harvard Medical School)/X. Wang (Indiana University) for providing plasmid templates pWX510 and pWX570. Support for this work came from the NIH (R35GM142460, S10OD026741) and the University of Washington Royalty Research Foundation.

## Author contributions

The project was conceived by M.C.W., A.E.R. and A.J.M. Experiments were performed by M.C.W., A.E.R. and A.J.M. Bioinformatic analysis was conducted by M.C.W., S.R.M. and A.J.M. J.L. and M.W. isolated *L. seeligeri* strains. Pilot microscopy experiments were performed with assistance from E.R.R. The paper was written and edited by M.C.W., A.E.R., S.R.M. and A.J.M.

## Competing interests

A.J.M. is a co-founder of Profluent Bio. The other authors declare no competing interests.

## Additional information

**Extended data** is available for this paper at https://doi.org/10.1038/s41564-022-01318-2.

**Supplementary information** The online version contains supplementary material available at https://doi.org/10.1038/s41564-022-01318-2.

**Correspondence and requests for materials** should be addressed to Alexander J. Meeske.

**Peer review information** *Nature Microbiology* thanks Mitchell O'Connell and the other, anonymous, reviewer(s) for their contribution to the peer review of this work

https://doi.org/10.1038/s41564-022-01318-2

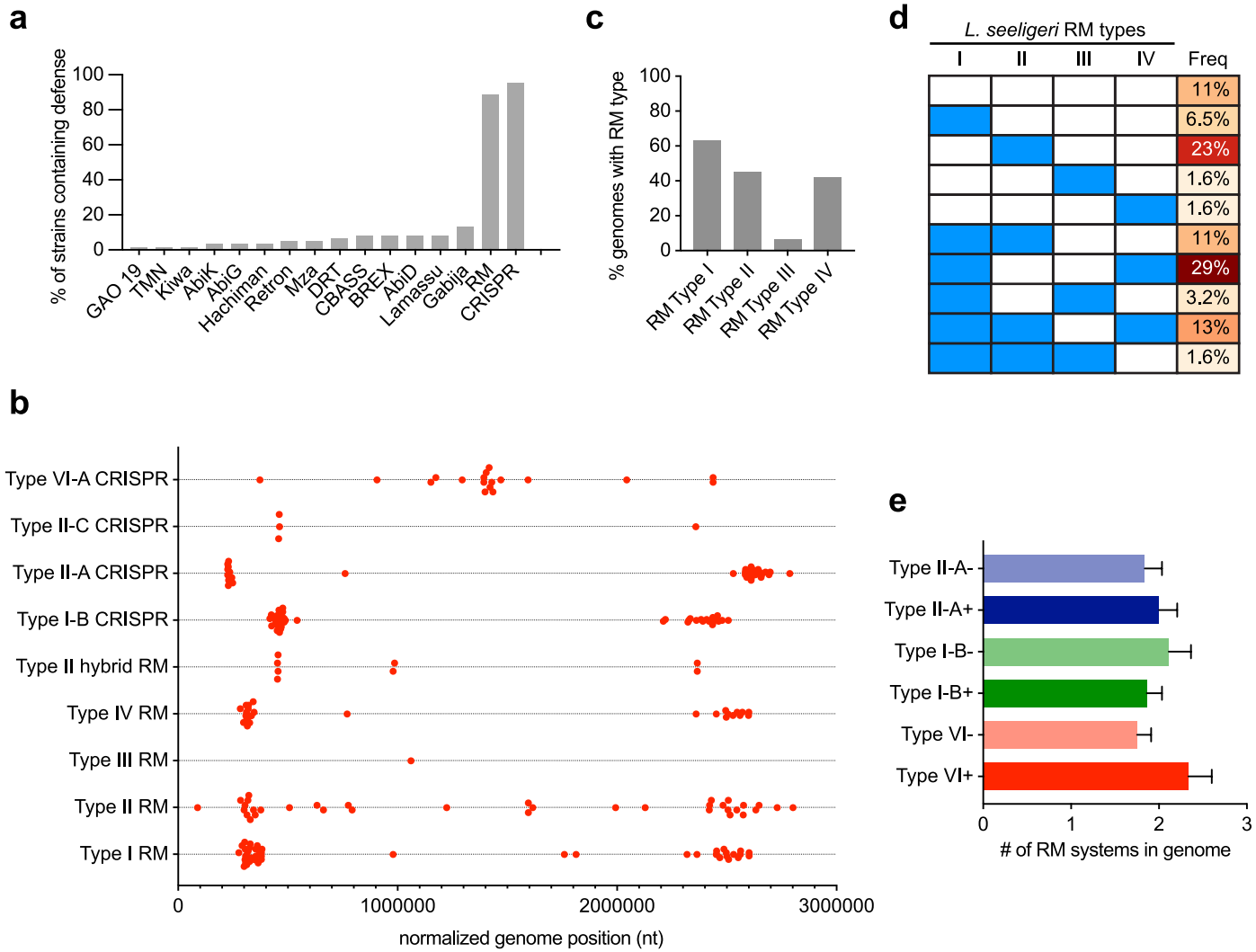


**Extended Data Fig. 1 | Bioinformatic analysis of anti-phage defenses in *L. seeligeri*.** **(a)** Anti-phage defense systems detected in 62 *L. seeligeri* strains using PADLOC. **(b)** Genomic locations of CRISPR and RM systems within all 62 *L. seeligeri* genomes. Each genomic location was normalized to the position of the well-conserved, origin-proximal *dnaA* gene. **(c)** Percentage of 62 *L. seeligeri* genomes harbouring the indicated RM type. **(d)** Combinations of RM types observed in 62 *L. seeligeri* genomes. Filled blue rectangles indicate the presence of the indicated RM type. **(e)** Tally of RM systems per genome in *Listeria* strains with or without the indicated CRISPR type. Error bars denote standard error of the mean.

https://doi.org/10.1038/s41564-022-01318-2

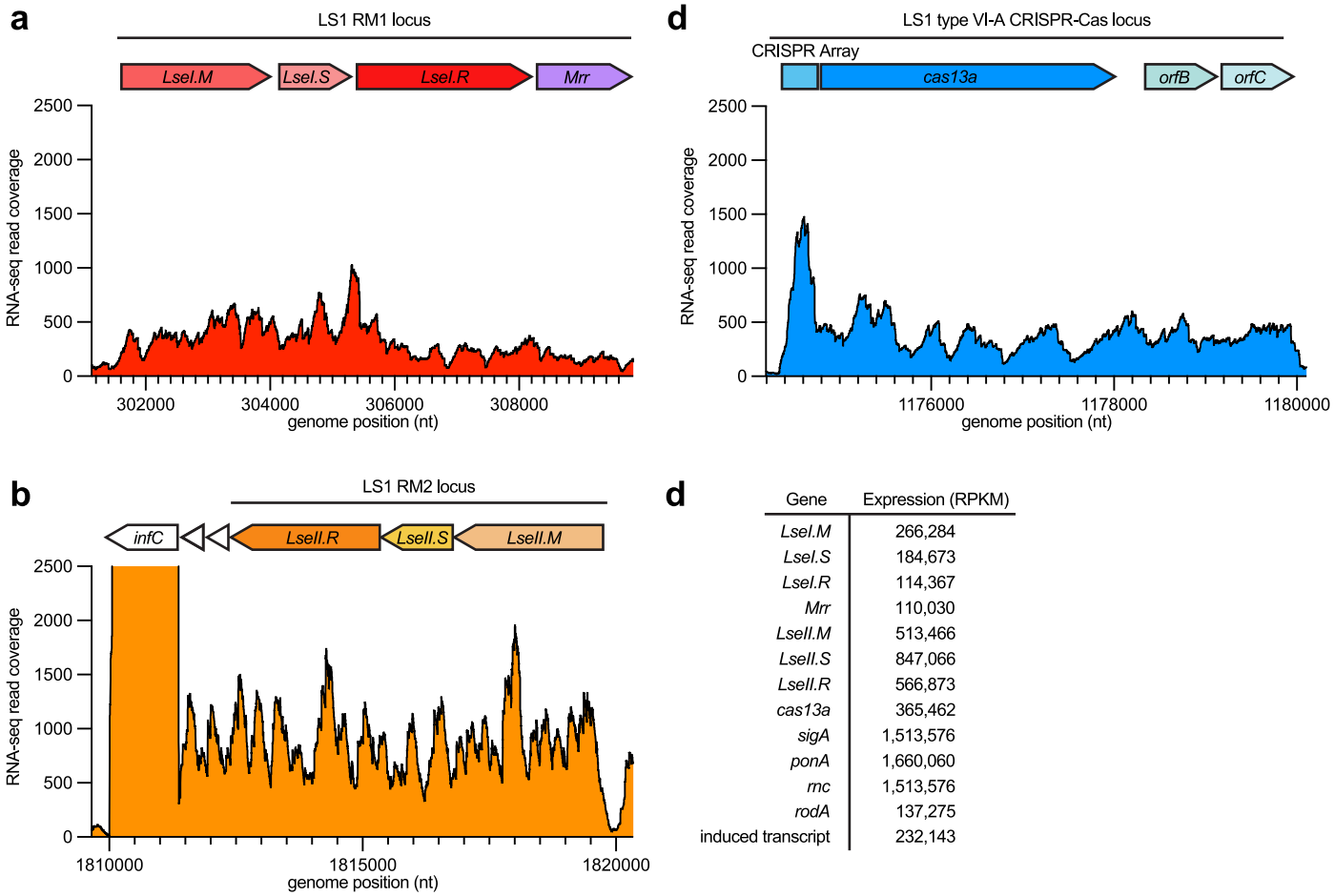


d

| Gene | Expression (RPKM) |
|---|---|
| *LselM* | 266,284 |
| *LselS* | 184,673 |
| *LselR* | 114,367 |
| *Mrr* | 110,030 |
| *LselI.M* | 513,466 |
| *LselI.S* | 847,066 |
| *LselI.R* | 566,873 |
| *cas13a* | 365,462 |
| *sigA* | 1,513,576 |
| *ponA* | 1,660,060 |
| *rnc* | 1,513,576 |
| *rodA* | 137,275 |
| induced transcript | 232,143 |

**Extended Data Fig. 2 | Both type I RM systems are expressed in *L. seeligeri* LS1. (a)**–**(b)** Diagrams of type I RM loci in the LS1 genome (methylase denoted M, specificity subunit denoted S, endonuclease denoted R, one locus also has a type IV nuclease denoted Mrr). RNA-seq read coverage at each nucleotide position of the two loci are plotted. The y-axis reflects the number of mapped reads overlapping each nucleotide position. **(c)** RNA-seq reads corresponding to the LS1 type VI-A CRISPR-Cas locus. **(d)** Table of expression values (RPKM, reads per kilobase per million mapped reads) for LS1 RM genes and *cas* genes, as well as essential genes *rodA, ponA, rnc, sigA*, and a transcript induced under Ptet control by the addition of aTc (anhydrotetracycline).

https://doi.org/10.1038/s41564-022-01318-2

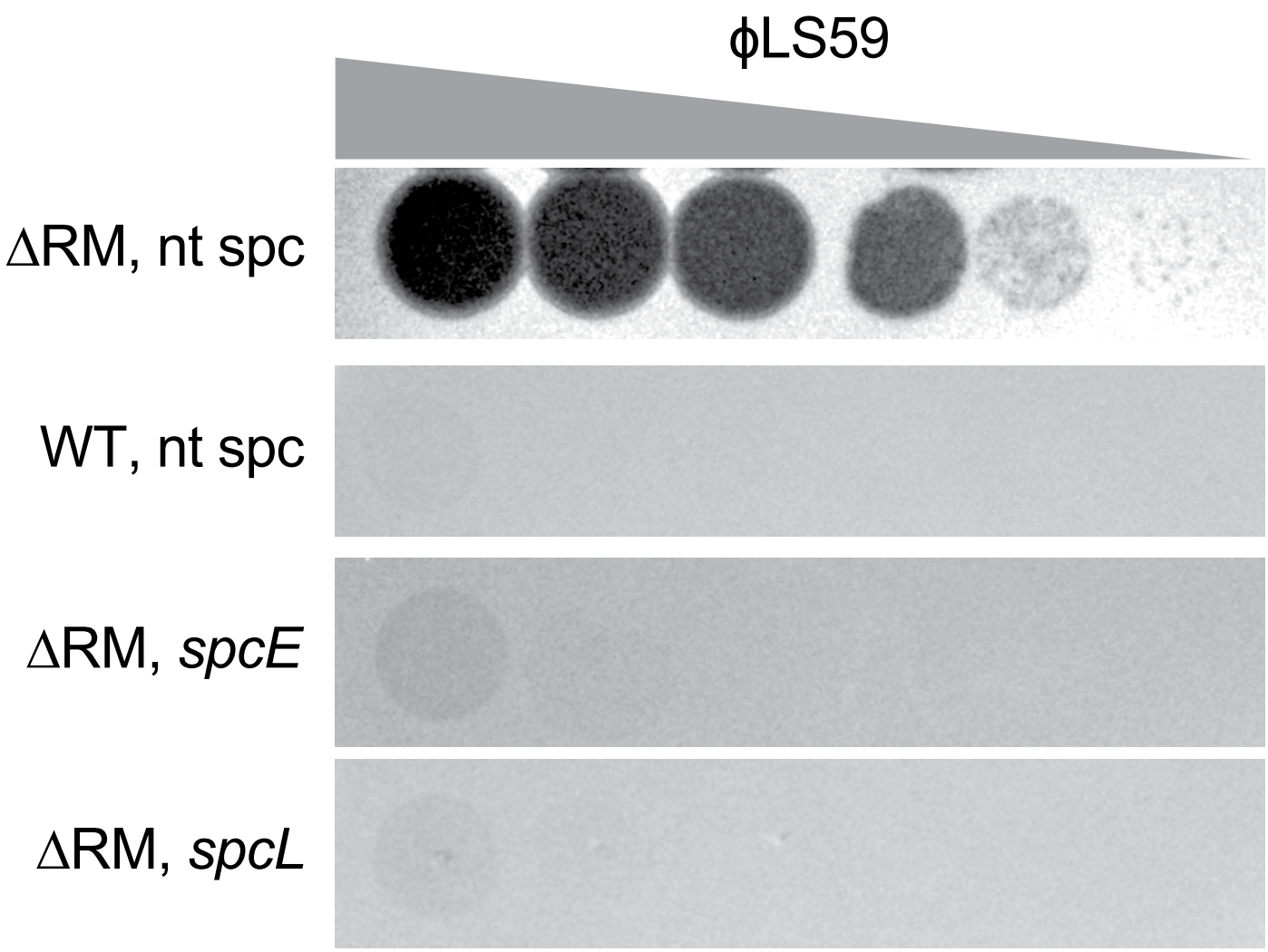


**Extended Data Fig. 3 | ϕLS59 is sensitive to both RM and type VI CRISPR immunity.** Plaque assay of ϕLS59 on a set of *L. seeligeri* strains lacking RM and type VI CRISPR immunity (ΔRM, nt spc), equipped with RM immunity only (WT, nt spc), or equipped with CRISPR immunity only targeting early lytic genes (ΔRM, *spcE*) or late lytic genes (ΔRM, *spcL*). Serial tenfold dilutions were made from the phage stock, and 2 µL of each dilution was spotted on the indicated bacterial lawn.

https://doi.org/10.1038/s41564-022-01318-2

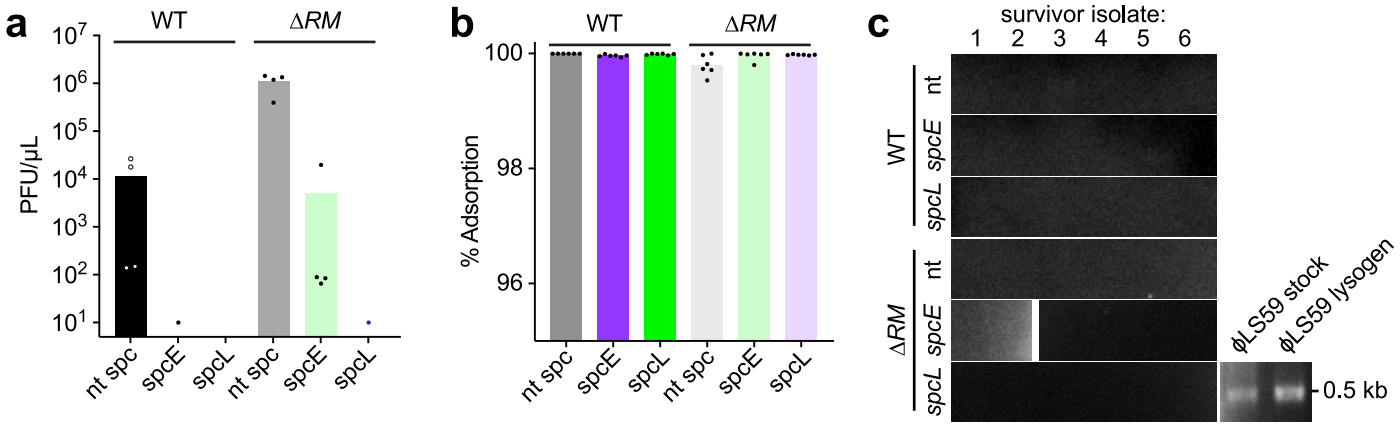


**Extended Data Fig. 4 | Clearance of phage and recovery of phage-sensitive cells after ϕLS59 infection. (a)** PFU titers from infection cultures shown in Fig. 3c at 24 hours post-infection. PFU were enumerated on a lawn of LS1 ΔRM nt spc. NT = non-targeting spacer, spcE = spacer targeting early lytic gene, spcL = spacer targeting late lytic gene. Analysis of 3 biological replicates is shown. **(b)** ϕLS59 adsorption assays performed on six surviving isolates from each the infections in Fig. 3c. **(c)** PCR with ϕLS59-specific primers performed on six surviving isolates from each of the infections in Fig. 3c, as well as positive control PCRs using the phage stock and a confirmed ϕLS59 lysogen.

https://doi.org/10.1038/s41564-022-01318-2

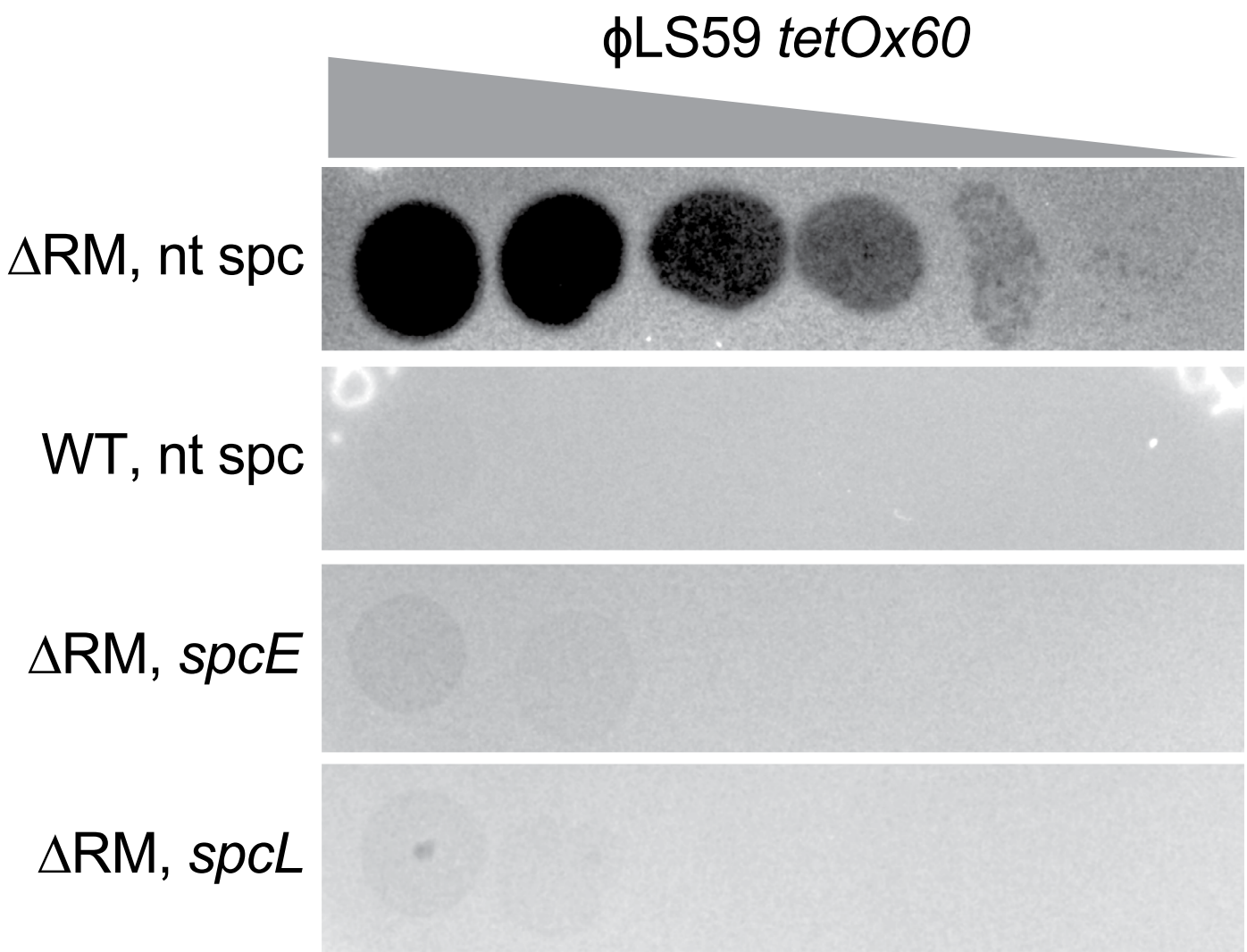


**Extended Data Fig. 5 | ϕLS59 tetOx60 is viable and sensitive to both RM and type VI CRISPR immunity.** Plaque assay of ϕLS59 *tetOx60* on a set of *L. seeligeri* strains lacking RM and type VI CRISPR immunity (ΔRM, nt spc), equipped with RM immunity only (WT, nt spc), or equipped with CRISPR immunity only targeting early lytic genes (ΔRM, *spcE*) or late lytic genes (ΔRM, *spcL*). Serial tenfold dilutions were made from the phage stock, and 2 µL of each dilution was spotted on the indicated bacterial lawn.

https://doi.org/10.1038/s41564-022-01318-2

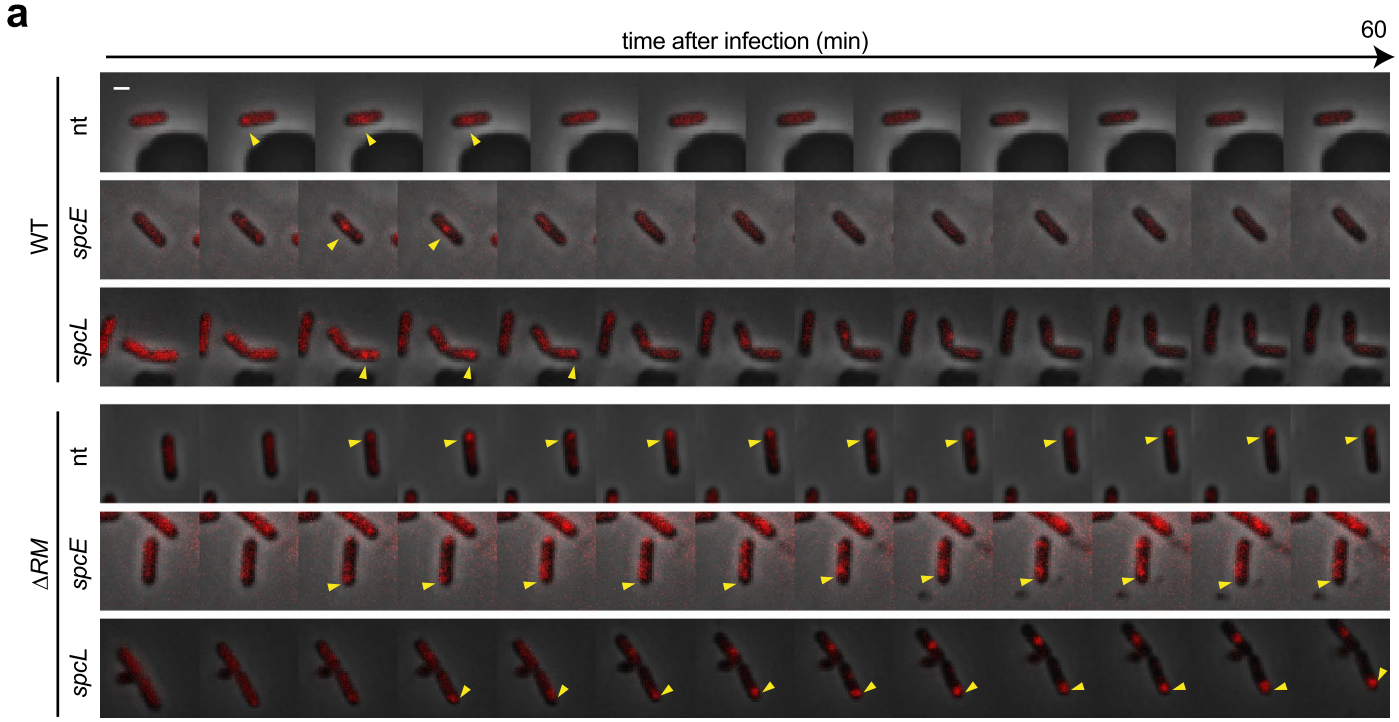


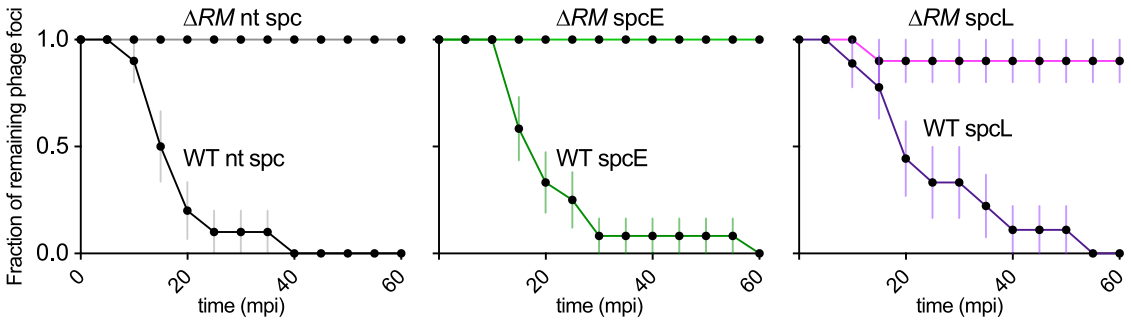


**Extended Data Fig. 6 | Kinetics of phage clearance by RM. (a)** Representative montage images from timelapse FROS experiments tracking ϕLS59 DNA during infection. LS1 cells with the indicated genotype harboring tetR-mCherry were infected with ϕLS59 tetOx60 and imaged every 5 minutes post-infection for 1 hour. Yellow carets indicate the presence of a phage DNA focus. Scale bar = 1 μm. **(b)** Quantitation of data in (a); percentage of cells that retained phage DNA foci at each time point after infection. Error bars represent standard error of the mean.

https://doi.org/10.1038/s41564-022-01318-2

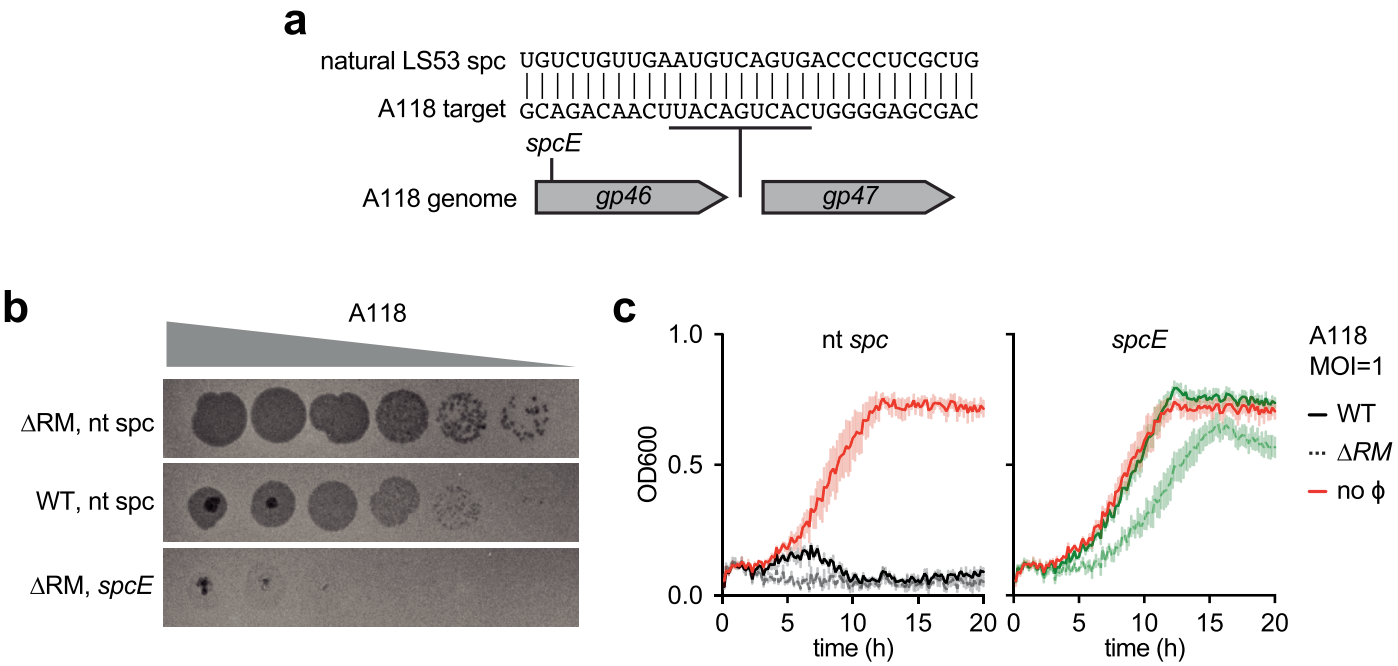


**Extended Data Fig. 7 | Phage A118 is sensitive to both RM and type VI CRISPR immunity. (a)** Region of the A118 genome targeted by natural and engineered type VI CRISPR spacers. **(b)** Plaque assay of A118 on on a set of *L. seeligeri* strains lacking RM and type VI CRISPR immunity (ΔRM, nt spc), equipped with RM immunity only (WT, nt spc), or equipped with CRISPR immunity only targeting early lytic genes (ΔRM, *spcE*). Serial tenfold dilutions were made from the phage stock, and 2 µL of each dilution was spotted on the indicated bacterial lawn. **(c)** Growth curves during A118 infection of LS1. Strains of the indicated genotype were infected at MOI = 1, OD600 = 0.01. OD600 was monitored for 20 hours after infection. Solid lines indicate wild-type, $RM^+$ strains, dashed lines indicate ΔRM strains. Uninfected controls are shown in red. Error bars are standard error of the mean from 3 biological replicates.

nature portfolio

Corresponding author(s): Alexander Meeske

Last updated by author(s): Dec 20, 2022

# Reporting Summary

Nature Portfolio wishes to improve the reproducibility of the work that we publish. This form provides structure for consistency and transparency in reporting. For further information on Nature Portfolio policies, see our Editorial Policies and the Editorial Policy Checklist.

## Statistics

For all statistical analyses, confirm that the following items are present in the figure legend, table legend, main text, or Methods section.

| n/a | Confirmed | |
|---|---|---|
| ☐ | ☒ | The exact sample size (*n*) for each experimental group/condition, given as a discrete number and unit of measurement |
| ☐ | ☒ | A statement on whether measurements were taken from distinct samples or whether the same sample was measured repeatedly |
| ☐ | ☒ | The statistical test(s) used AND whether they are one- or two-sided<br>*Only common tests should be described solely by name; describe more complex techniques in the Methods section.* |
| ☒ | ☐ | A description of all covariates tested |
| ☒ | ☐ | A description of any assumptions or corrections, such as tests of normality and adjustment for multiple comparisons |
| ☐ | ☒ | A full description of the statistical parameters including central tendency (e.g. means) or other basic estimates (e.g. regression coefficient) AND variation (e.g. standard deviation) or associated estimates of uncertainty (e.g. confidence intervals) |
| ☐ | ☒ | For null hypothesis testing, the test statistic (e.g. *F*, *t*, *r*) with confidence intervals, effect sizes, degrees of freedom and *P* value noted<br>*Give P values as exact values whenever suitable.* |
| ☒ | ☐ | For Bayesian analysis, information on the choice of priors and Markov chain Monte Carlo settings |
| ☒ | ☐ | For hierarchical and complex designs, identification of the appropriate level for tests and full reporting of outcomes |
| ☐ | ☒ | Estimates of effect sizes (e.g. Cohen's *d*, Pearson's *r*), indicating how they were calculated |

*Our web collection on statistics for biologists contains articles on many of the points above.*

## Software and code

Policy information about availability of computer code

| | |
|---|---|
| Data collection | Microscopy data was collected using NIS Elements software (v5.3). Northern blot images were acquired using Azure Biosystems Sapphire control software (v1.0). |
| Data analysis | Microscopy data was processed using NIS Elements software (v5.3), then analyzed using Fiji (v2.3.0). Contrast of northern blot images was adjusted in Fiji (v2.3.0). Growth curves, CFU and PFU measurements, and bioinformatic data were analyzed in GraphPad Prism 9. PacBio sequencing data was analyzed with SMRTLink SMRTAnalysis toolbox (v10.1.0.119588). Genome assembly was performed with Sickle v1.0, SPAdes v.3.15.4, and Medusa webserver (no version provided). |

For manuscripts utilizing custom algorithms or software that are central to the research but not yet described in published literature, software must be made available to editors and reviewers. We strongly encourage code deposition in a community repository (e.g. GitHub). See the Nature Portfolio guidelines for submitting code & software for further information.

## Data

Policy information about availability of data

All manuscripts must include a data availability statement. This statement should provide the following information, where applicable:

- Accession codes, unique identifiers, or web links for publicly available datasets
- A description of any restrictions on data availability
- For clinical datasets or third party data, please ensure that the statement adheres to our policy

All L. seeligeri genome sequences reported here have been uploaded to NCBI through Genbank under BioProject accession number PRJNA901958. RM loci are publically available through the REBASE database (rebase.neb.com). Lists of strains, plasmids, and oligonucleotides used in this study are available in Supplementary Table 2. Further information and requests for resources and reagents should be directed to and will be fulfilled by the corresponding author, Alexander Meeske (meeske@uw.edu).

## Human research participants

Policy information about studies involving human research participants and Sex and Gender in Research.

| | |
|---|---|
| Reporting on sex and gender | N/A |
| Population characteristics | N/A |
| Recruitment | N/A |
| Ethics oversight | N/A |

Note that full information on the approval of the study protocol must also be provided in the manuscript.

# Field-specific reporting

Please select the one below that is the best fit for your research. If you are not sure, read the appropriate sections before making your selection.

☒ Life sciences ☐ Behavioural & social sciences ☐ Ecological, evolutionary & environmental sciences

For a reference copy of the document with all sections, see nature.com/documents/nr-reporting-summary-flat.pdf

# Life sciences study design

All studies must disclose on these points even when the disclosure is negative.

| | |
|---|---|
| Sample size | Sample sizes were not statistically predetermined. All experiments were performed with sample sizes based on standard protocols in the field. |
| Data exclusions | No data were excluded from the analysis. |
| Replication | All experimental findings were reliably replicated in biological triplicate. |
| Randomization | Not relevant to this study. Animal or human research subjects were not involved in this study. |
| Blinding | Not relevant to this study. Animal or human research subjects were not involved in this study. |

# Reporting for specific materials, systems and methods

We require information from authors about some types of materials, experimental systems and methods used in many studies. Here, indicate whether each material, system or method listed is relevant to your study. If you are not sure if a list item applies to your research, read the appropriate section before selecting a response.

## Materials & experimental systems

| n/a | Involved in the study |
|---|---|
| ☒ | ☐ Antibodies |
| ☒ | ☐ Eukaryotic cell lines |
| ☒ | ☐ Palaeontology and archaeology |
| ☒ | ☐ Animals and other organisms |
| ☒ | ☐ Clinical data |
| ☒ | ☐ Dual use research of concern |

## Methods

| n/a | Involved in the study |
|---|---|
| ☒ | ☐ ChIP-seq |
| ☒ | ☐ Flow cytometry |
| ☒ | ☐ MRI-based neuroimaging |